CORONAL SIGNATURES OF ACCELERATED ELECTRONS

G. Trottet[1]

[1]*Observatoire de Paris–Meudon (LESIA), 5, Place J. Janssen F92190 Meudon, France*

ABSTRACT

Whereas hard X-rays, microwaves and gamma-rays trace flare accelerated electrons and ions interacting in the low corona and the chromosphere, imaging and spectral radio observations in the decimetric-dekametric domain provide signatures of non thermal electrons in the middle and upper corona. These latter radio observations, combined with X-ray, EUV and optical measurements, contain unique information on the various circumstances of electron acceleration whether they are associated with flares or not. In this paper we outline the results of multiwavelength studies which provide: (i) information on the magnetic structure at various spatial scales into which flare accelerated electrons are injected/accelerated and (ii) evidence for various sites of electron acceleration outside flares which are located in the corona at altitudes ranging typically from ~ 0.1 to $\sim 1\ R_\odot$ above the photosphere.

INTRODUCTION

The behavior of the solar corona is governed by the interplay between magnetic fields and plasmas which drives magnetic energy conversion leading to the production of energetic particles at all energies. Suprathermal particles are thus an essential key for understanding energy release in the solar atmosphere. Observations accumulated over the past few decades have shown that particle acceleration does not occur only in flares. Indeed, the production of particles is also associated with a variety of energy release events recognizable at e.g., UV and X-ray wavelengths, but unaccompanied by the clear signature at optical wavelengths commonly used to define a flare. While energetic ions produce gamma-ray (GR) lines and high-energy gamma-ray continuum emission when they interact with the photosphere and chromosphere, interacting electrons produce radiative signatures in the whole electromagnetic spectrum, i.e. over a large domain of altitudes ranging from the upper chromosphere to the high corona and interplanetary space. Multiwavelength studies thus provide a comprehensive approach to understanding particle acceleration and transport in the solar atmosphere.

Hard X-ray (HXR), GR and millimetric–short-decimetric radio observations are discussed elswhere in these proceedings. Here we focus on radio observations obtained at long decimetric and longer wavelengths with emphasis on imaging observations made by the Nançay radioheliograph (NRH) in the 0.7–2 m wavelength range (450–150 MHz). Such radio diagnostics constitute the most sensitive signatures of keV-electrons at coronal altitudes ranging from about a few times 10^4 to a few times 10^5 km above the photosphere. The comparison of these data with measurements obtained in other spectral domains provide a unique way to investigate the large scale magnetic structure in which accelerated flare electrons radiate and to discuss the sites and circumstances of the production of suprathermal electrons in the absence of flare.

ENERGETIC ELECTRONS PRODUCED DURING FLARES

Multiwavelength studies combining HXR and radio observations have provided evidence that two distinct episodes of electron acceleration may occur during a flare: acceleration in the low corona, as traced by the HXR and millimetric–centimetric emission, followed, in some but not all flares, by time extended acceleration (tens of minutes to hours) which starts 10 to 20 mn after the flare onset during the decay of or even after the HXR emission (e.g. Pick, 1986; Trottet, 1986).

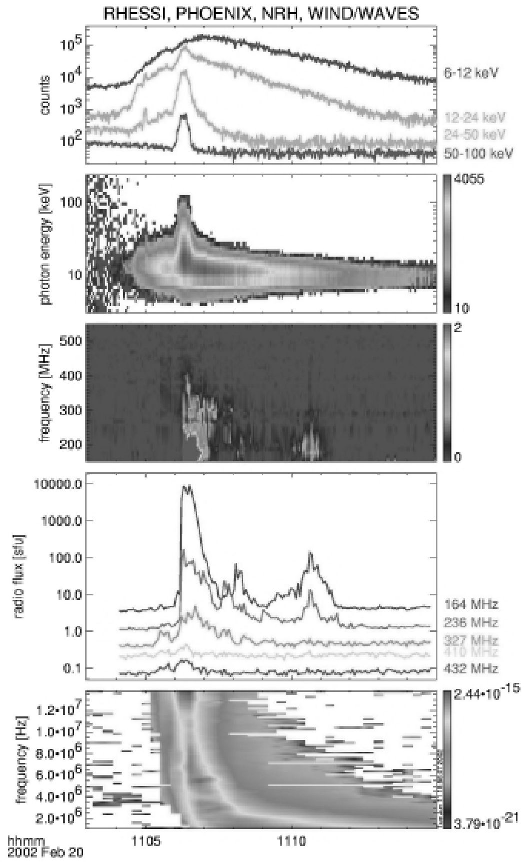

Fig. 1. X-ray and radio observations of the 2002 February 20 flare at ~ 11:06 UT (after Vilmer et al., 2002). From top to bottom: time evolution of the 6-100 keV X-ray emission in four energy bands; spectrogram showing the time evolution of the energy of the X-ray photons; radio spectrum between 550 and 150 MHz; total radio fluxes at 164, 236, 327, 410 and 432 MHz divided respectively by 1, 5, 15, 75 and 150; radio spectrum between 12 and 2 MHz.

Joint studies of HXR and radio decimetric observations have provided convincing evidence that the bulk of electrons producing these radiations is accelerated in the low corona at heights around 10^4 km and medium densities ranging from $\sim 10^9$ cm^{-3} to $\sim 10^{11}$ cm^{-3} (e.g. Benz and Kane, 1986; Aschwanden et al., 1995). This is consistent with X-ray imaging observations of a few flares which suggest that energy release may appear either near the top of $\sim 10^4$ km magnetic loops, possibly in the cusp region one would find in an arcade of post flare loops (e.g. Takakura et al., 1993) or close to the interaction region between loops or loop sytems of different sizes, typically 10^4 km and a few times 10^4-10^5 km (e.g. Hanaoka, 1999). However, a significant fraction (10%–15%) of the HXR producing flares have no detectable emission at decimeter and longer wavelengths (Simnett and Benz, 1986). This suggests that, for these flares, electrons were accelerated and confined in low lying loops with no access to the higher corona (e.g. Rieger et al., 1999).

While HXR and microwaves constitute quantitative diagnostics of electrons injected in low lying loops, radio emission at long decimetric and hectometric wavelengths traces electron trajectories over a wide domain of altitudes ranging from $\sim 0.1\ R_\odot$ to a few $R_\odot$ above the photosphere. Studies combining radio spectral measurements and NRH imaging observations with HXR/GR spectral and occasional imaging observations (e.g. Raoult et al., 1985; Chupp et al., 1993; Trottet et al., 1994, 1998; Raulin et al., 2000; see also Trottet and Vilmer, 1997; Vilmer and Trottet 1997 for reviews) have revealed that:

1. Despite some differences, the radio and HXR time profiles bear remarkable similarities. This is illustrated in Figure 1, from Vilmer et al. (2002), which shows that > 50 keV X-rays and the most intense part of the radio emission below ~ 410 MHz start simultaneously and have similar durations. This is an indication that HXR and radio emitting electrons are produced at common acceleration sites.

2. Electrons are injected from these acceleration sites in both open flux tubes where they radiate type III bursts, signatures of upward moving electron beams (radio emission below 12 MHz in Figure 1), and large scale loops ($\sim 10^5$ km) where they produce broad-band contina (type V, type IV bursts), signatures of partially trapped electrons.

3. The spatial distribution of the radio emitting sources is complex and strongly evolves on time scales of a few seconds. This is illustrated in Figure 2 from Raulin et al. (2000) for a weak flare (GOES C2.6). The bars show the regions covered by the ensemble of radio emitting sources detected at each NRH observing frequency overlaid on a full-disk soft X-ray (SXR) image obtained with the Soft X-ray Telescope (SXT) on board *YOHKOH*. SXR images, obtained in a smaller field of view during the flare, provided evidence that energy release was

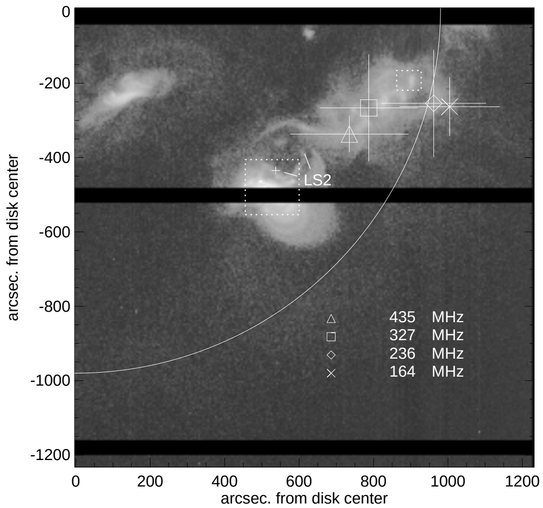

Fig. 2. X-ray and radio observations of the 1992 October 28 flare at ~ 10:07 UT (after Raulin et al., 2000). Extensions of the decimeter-meter radio emitting regions (bars) superimposed on a SXR image. Dotted boxes show the locations of two active regions and the small cross indicates the position of a compact SXR loop system near one leg of a more extended one marked LS2 (see text).

due to the interaction of a compact loop system marked by a cross and a larger one referred to as LS2. The general organization of the radio regions indicates that the emitting electrons were most probably injected into a complex of large scale loops connecting the flare site to a remote active region. However, within each emitting region there were several radio sources and their spatial distribution was found to vary on time-scales of a few seconds. This is an indication that electrons are successively injected into different flux tubes of the highly inhomogeneous large scale loop system, and that electron trajectories within this loop complex changed with time. By contrast, during the whole event, the HXR emission was produced in a compact source spatially associated with the compact SXR loop system. Figure 3 , from Vilmer et al. (2002), shows the spatial distribution and the time evolution of the three footpoint sources (marked 1 to 3 on the figure) and of the looptop source detected above 30 keV by RHESSI during a C7.5 flare. Figure 4 shows the radio emission pattern observed at 410 MHz by the NRH and the 25–40 keV HXR sources detected by RHESSI at two different times. The HXR emission exhibits two peaks of similar intensity. While source 1 was the brightest during the first HXR peak, during the second peak source 3 is the most intense.

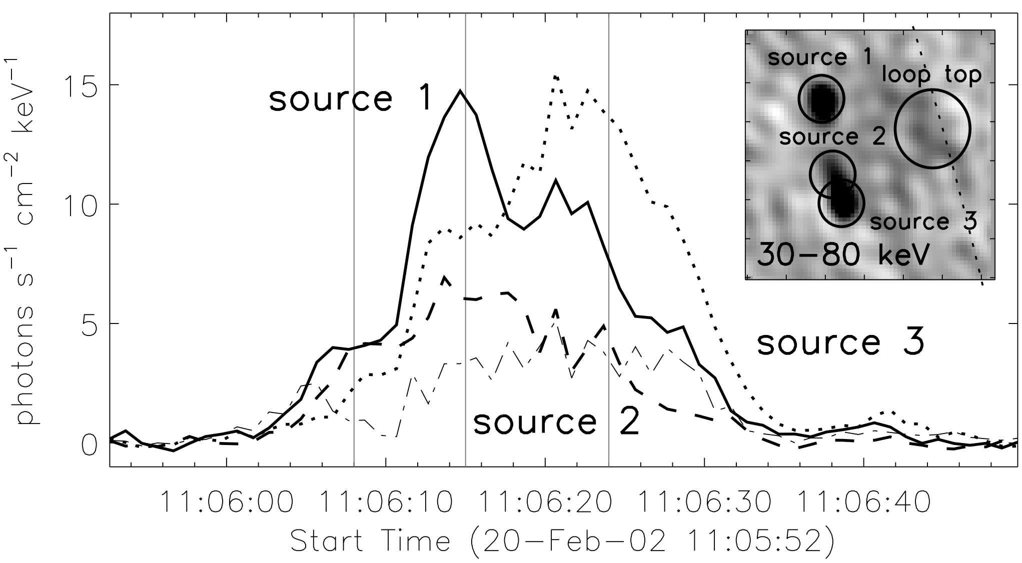

Fig. 3. Time evolution of the different 30–80 keV HXR sources detected by RHESSI during the 2002 February 20 flare (after Krucker and Lin, 2002

This change in the pattern of the HXR sources is accompanied by simultaneous modifications of the radio source distribution which correspond to a noticeable change of the relative intensity of the two sources detected

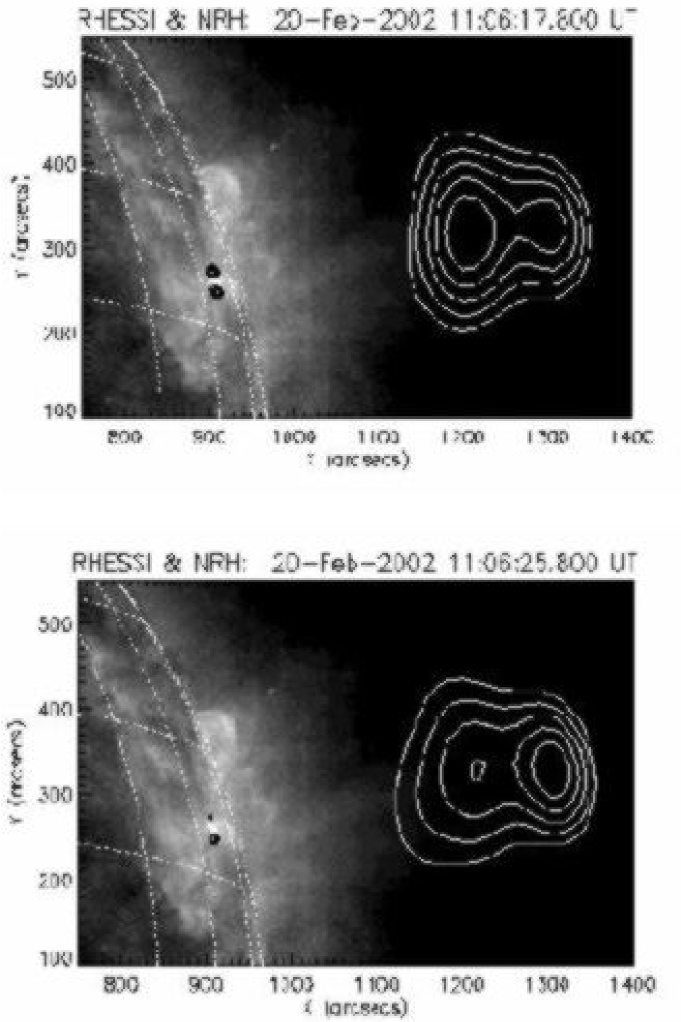

Fig. 4. 2002 February 20 flare: 25–40 keV HXR sources (black iso-contours) and 410 MHz sources (white iso-contours) at 11:06:17 UT (top panel) and 11:06:25 UT (bottom panel) superposed on an EIT image obtained at 11:12 UT. (adapted from Vilmer et al., 2002)

at 410 MHz. This is in line with the results of Raulin et al. (2002), although the radio source distribution is much less complex and the HXR source pattern more complex than those reported in Raulin et al. (2000).

These two examples and similar results obtained for other flares, including GR line and electron-dominated events, provide convincing evidence that electron acceleration may occur at sites, the locations of which vary on time scales of a few seconds within the energy release volume. This is in line with HXR observations of one flare which revealed that succesive HXR peaks resulted from successive energy release in different loops (Sakao et al., 1992). However, the spatial resolution and/or the dynamical range of HXR imagers are not sufficient to resolve the small scale where energy conversion takes place.

4. Stepwise changes of the spectral characteristics of energetic electrons inferred from HXR spectral measurements were found to be closely associated with changes of the spatial distribution of the radio emitting sources i.e. with changes of the magnetic structures into which electrons are injected from the acceleration site. This shows the role of the magnetic environment on the characteristics of the energetic electrons and thus on the efficiency of the different acceleration and transport processes.

Time-extended Acceleration following Flares

Ten to twenty minutes after a flare onset, long lasting (tens of minutes to hours) radio signatures of supra thermal electrons may be observed from decimetric to dekametric wavelengths, that is typically between 0.1 and 1 $R_\odot$ above the photosphere. This late radio emision has no detectable HXR counterpart. It is generally associated with flares occuring in large and complex active regions which are often accompanied by large scale disturbances such as: CMEs, filament eruptions and coronal shock waves revealed by radio type II bursts. Because coronal type II shocks play a minor role, if any, in this long-lasting production of electrons (Klein et al., 1983, 1989) and because there are no detectable signatures of these electrons in the low atmophere, acceleration must take place at higher altitudes than during the HXR emission (e.g. Trottet, 1986). The spatial distribution of the radio emitting sources is consistent with complex acceleration sites emcompassing diverging magnetic field lines and large scale loops and may spread over an area comparable to that spanned by a CME. However, these acceleration sites are located far behind the CME leading edge (Maia et al., 1999; Klein et al., 1999a, 2001). It was suggested that electron acceleration results from reconnection of large scale coronal structures previously opened by the passage of an eruptive prominence or a CME (e.g. Švestka and Cliver, 1992). Such an environment allows electrons rapid access to the outer corona and interplanetary space. Assuming that electrons are representative of charged particles as a whole, it has been argued that well-connected sites of coronal acceleration may significantly contribute to particle fluxes detected at 1 A.U. in the interplanetary space and at the Earth's ground level (Klein et al., 1999a, 2001; Laitinen et al., 2000; Trottet and Klein, 2000). However, due to the lack of unique and quantitative modeling of radio emitting sources, an estimate of the importance (energetically) of such a possible contribution remains out of reach at present.

ACCELERATION OF ELECTRONS OUTSIDE FLARES

The production of electrons in the absence of a flare or not directly associated with flares refers to events with comparatively low energy budget or without detectable signatures of energy input in the low atmosphere (see Klein, 1994; 1998 for reviews). In the following we outline some results of multiwavelength studies relevant to the production of electron beams and to the occurrence of time-extended (tens of minutes to days) acceleration of electrons in the absence of flares.

Spikes and Type III Bursts at Metric Wavelengths

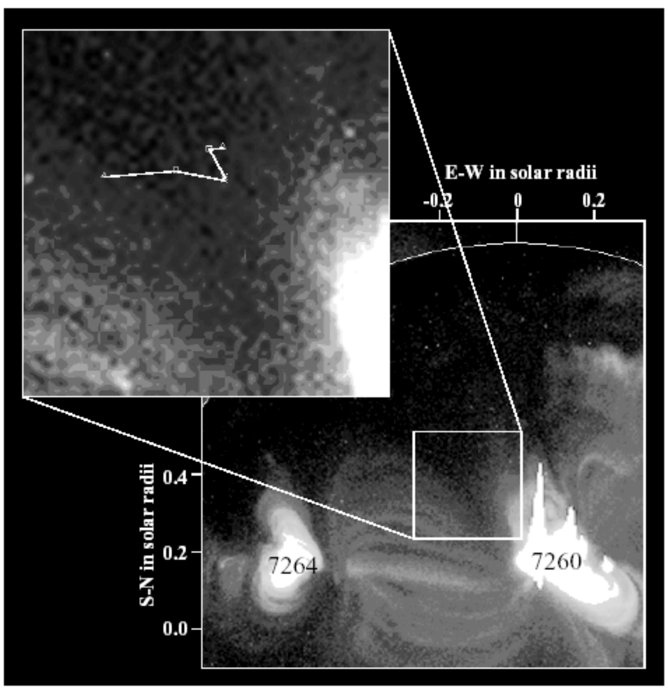

Fig. 5. Projected trajectories of two divergent type III bursts during the 1992 August 18 event at 14:14 UT overlaid on a Yohhoh SXT image taken with the Al.1 filter at 16:29:07 UT (after Paesold et al., 2001).

Radio spikes are short (few tens of ms) and narrow band (few percent of the center frequency) bursts that are a signature of coherent emission by electrons. Whereas decimetric spikes are suspected to be related to the energy release process in flares (e.g. Aschwanden, 2002 and references therein), in the metric domain, there are spike events which occur in the absence of flares and which are closely associated with type III's starting at a slightly lower frequency (e.g. Benz et al., 1996). Earlier imaging investigations of metric spikes associated with type III's (Krucker et al., 1995, 1997) found spike sources at high altitudes and suggested that the spike source could be the acceleration region of type III electron beams. More recently Paesold et al. (2001) have produced convincing evidence that supports this suggestion by combining spectral and multi-wavelength imaging observations of four metric spike-type III events. Indeed, extrapolation to lower altitudes of the type III trajectories inferred from the NRH images are in close coincidence with the location of the associated spike source. Moreover, Paesold et al. (2001) observed separate type III's in the same group which follow divergent paths from the same spike source. Figure 5 shows that, when overlaid on the SXT image taken at a time close to that of the radio event, the starting positions of these divergent type III's are near a location where the connectivity of field line changes, i.e. a key location in the occurrence of magnetic reconnection. However, whether spikes are a signature of a highly fragmented acceleration process or of their radiation process and whether they come from the acceleration region or from its immediate vicinity remain important questions for sorting out what spikes tell us about electron acceleration.

Electron Beams Associated with Ejecta in the Low Corona

The production of type III electron beams in association with jets of material in the low atmosphere has long been known from Hα and radio observations (Chiuderi-Drago et al., 1986 and references therein). The type III bursts are not observed at the launch of the Hα material, but most often around the time when its line-of-sight velocity is the greatest. This association does not appear systematic, only Hα jets located at the border of an active region or near a line of photospheric magnetic field reversal have associated type III bursts (Axisa et al., 1973). The global magnetic field structure associated with an active region thus plays a key role in determining whether a jet of cool material is accompanied by electron beams in the overlying corona or not. More recently, electron beams were observed in conjonction with the expulsion of hot plasma visualized as SXR jets (Aurass et al., 1994; Kundu et al., 1995; Raulin et al. 1996; van Driel-Gesztelyi et al., 1998). Given that only a few single case studies of such an association exist it is not possible to draw a general picture of such a phenomenon. For example, the jet studied by Kundu et al. (1995) started in the vicinity of an X-ray bright point in the outskirts of an active region and was associated with a single type III burst. This type III burst occurred at about the time when the ejected plasma reached the projected position of the high-frequency radio source (236 MHz) and electron densities inferred from the radio and X-ray data were consistent. This would be in agreement with acceleration near the front of the jet. However in at least one case, the electron beams were found to propagate through the already existing jet of material. Therefore, they could not have been accelerated at its front (Raulin et al., 1996). The electrons rather seem to be accelerated near the base of the jet , but minutes after the plasma has been ejected. A possible site for the acceleration of the plasma jet and of the electron beams is the region of interaction between an emerging magnetic flux and the ambient magnetic field structures. This is generally observed at the base of surges and SXR jets (e.g. Chiuderi-Drago et al. 1986; Shibata, 1997 and references therein). Such a suggestion is supported by the case study by Aurass et al. (1994) where a SXR jet, elongated at its base, was found to be associated with beams injected in both open (type III burst) and closed (type U burst) field lines. Indeed, the close temporal and spatial association between the plasma jet and the beams revealed by the radio measurements is consistent with acceleration of the jet and of the beams at the interface between regions of different magnetic connectivity.

Two possibilities seem to be consistent with all reported case studies: energy release at the base of the jet, i.e. through magnetic reconnection between emerging flux and preexisting structures and internal instabilities of the jet (Carbone et al., 1987). Both interpretations require that electron acceleration occurs at the interface of different magnetic structures. The latter one further predicts a close link between the deceleration of the jet and electron acceleration. In agreement with this, Kundu et al. (1995) found indications that the speed of the plasma jet has started to decrease when type III's are observed.

Electron Acceleration in the Middle and High Corona

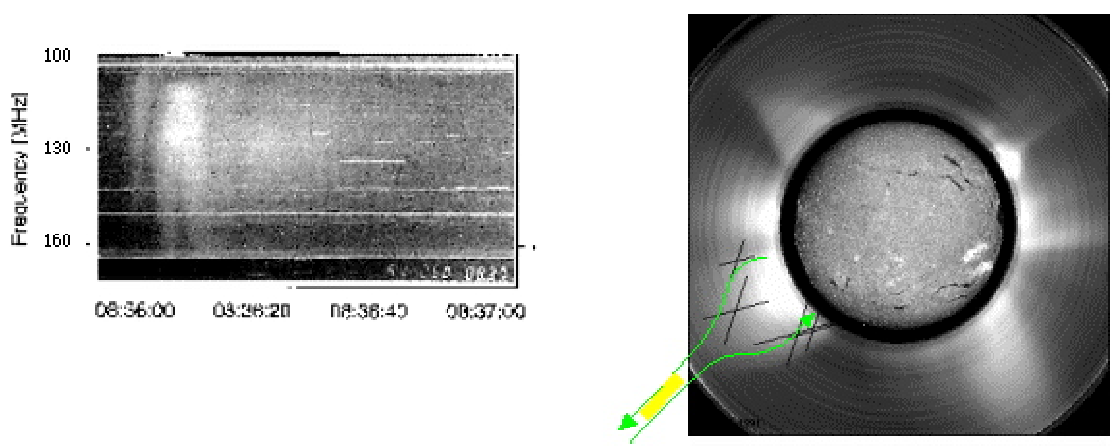

Fig. 6. Left: radio spectrum (100-170 MHz) of two reverse drift bursts. Right: locations of the two reverse drift bursts at 164 MHz on top of a Mauna Loa image of the white light corona taken 15 hours before the bursts. The location of the current sheet of the coronal streamer inferred from the burst positions is also shown schematically (after Klein et al., 1997).

Electron beams which are produced at coronal altitudes above roughly 0.5 $R_\odot$ (type III starting frequency $\leq$

100 MHz) are a frequent counterpart of complex active regions with noise storm emission at meter wavelengths. At 1 A.U., the most frequent transient electron populations of solar origin are electron beams detected up to ~ 10 keV (e.g. Lin, 1985, 1997). Since their observed power law spectra extend most often down to 2 keV without any signature of Coulomb energy losses, the acceleration sites of these beams must be in a tenuous plasma, at heights greater than 0.2–0.5 $R_\odot$ (Lin, 1985, 1997). These electron populations are produced without major energy release in the low atmosphere and with no signatures of coronal shocks. On theoretical grounds Gubchenko and Zaitsev (1983) and Cliver and Kahler (1991) have suggested that the current sheet of a coronal streamer may be an adequate site of acceleration. This is supported by a case study by Klein et al. (1997) of reverse slope (RS) bursts, signatures of electron beams travelling downward through the corona. Figure 6 (left) shows the spectrum of two RS bursts observed in the 100–170 MHz frequency range. Figure 6 (right) shows that when mapped at 164 MHz (i.e. close to their high-frequecy limit), each RS burst corresponds to the simultaneous brightening of two sources with projected locations, separated by $\sim 0.7\ R_\odot$ (crosses), on both sides of a coronal streamer. These observational facts led the authors to conclude that electrons where accelerated in a rather small volume at $\sim 1\ R_\odot$ above the photosphere and injected along magnetic field lines which separate at lower altitudes. This is consistent with acceleration in the current sheet of a coronal streamer as schematized in Figure 6 (right).

Time-Extended Acceleration Associated with Ejecta

Ejections of hot plasma as jets or plasmoids are not only associated with electron beam production but may also drive time-extended acceleration seen as wide-band radio decimetric-metric continua. Kundu et al. (2001) reported two such cases of SXR plasmoids, with speeds in the 100–200 km s^{-1} range, associated with two limb flares. The radio emission observed in the 150–450 MHz range by the NRH was a continuum which lasted 8–10 mn in one case and about 120 mn in the second case. The radio sources were located above the SXR ejecta, in the general direction of the prolongation of the ejecta motions. In one case, the high-frequency source (410 MHz) onset occurred at a location where the plasmoid was last identified in SXT images. Moreover, the onset time of the low-frequency continuum was delayed with respect to its onset at higher frequencies. A plausible interpretation, drawn by Kundu et al. (2001), is that as the plasmoid moves to higher altitudes its interaction with increasingly more extended magnetic structures creates, due to e.g. magnetic reconnection, new coronal sites of electron acceleration. It should be noticed that much faster SXR ejecta (700–900 km s^{-1}) may also drive large scale coronal shocks seen as radio type II bursts (Gopalswamy et al., 1997; Klein et al., 1999b).

Klein and Mouradian (2002) have reported an erupting prominence and a moving metric type IV source which trace a common magnetic structure during its rise from $\sim 10^3$ km to 3 $R_\odot$ above the limb. Electrons were accelerated in the surroundings of the rising structure and in two flares up to 70 degrees away from the prominence. Due to the close temporal association and the existence of transequatorial loops, there may be some physical link between the acceleration of electrons in remote regions and the prominence ejection, but the authors found no evidence for a triggering of one by the other: the erupting prominence and the flares may be manifestations of localized energy conversion within a large scale instability that implies multipolar magnetic structures (e.g. Aulanier et al., 2000). A plausible possibility is that electrons radiating the moving type IV were accelerated in the current sheet which formed underneath the rising structure (Klein and Mouradian, 2002).

Time-Extended Acceleration Associated with non Flaring Active Regions

The oldest signatures of time-extended acceleration of electrons in the corona are radio noise storms. Noise storms are associated with active regions, sometimes with flares and CMEs, but occur most often without conspicuous activity in the underlying atmosphere and last (hours to days) much longer than flares. The noise storm radio spectrum comprises a broadband decimetric-metric continuum ($\Delta\nu/\nu \sim 1$) and short-lived (< 1 s) and narrow-band ($\Delta\nu/\nu \leq 0.03$) type I bursts. Comprehensive reviews of noise storm observations and theories were given in Elgarøy (1977) and in Kai et al. (1985). Briefly stated, the radio emission implies collective processes from partially trapped electrons producing electromagnetic waves at the local electron plasma frequency. The energy of radiating electrons was estimated to be in the range of a few keV to a few tens of keV (e.g. Raulin and Klein, 1994). The life time of these electrons against Coulomb collisions being of a few tens of seconds, electrons have to be accelerated throughout the whole noise storm duration. The rate of energy release has been estimated to be of the order of 10^{23}–10^{25} erg s^{-1} (cf. Klein, 1998 and references therein). Noise storms are therefore signatures of nonthermal processes involving small rates of energy release related to the global and slow evolution of coronal structures in the middle corona. However, noticeable structural changes of the corona are seen prior to or at the onset of noise storms. These include:

(i) a restructuring of the corona seen as brightenings of narrow features in white light observations (Kerdraon et al., 1983); (ii) reconfiguration of active regions on timescales of a few minutes to tens of minutes revealed by microwave and SXR observations (Raulin et al., 1991; Raulin and Klein, 1994) and (iii) electron acceleration up to tens of keV in the low corona producing non thermal X-ray bursts which last $\sim$ 10 mn (Crosby et al. 1996). The X-ray and microwave signatures at the beginning of noise storms are reminiscent of weak flares and indicate that the onset of noise storms is related to energy conversion in the associated active region. However, on time scales of a few minutes to a few tens of minutes the radio signatures shift to lower frequencies, i.e. to more dilute regions, at typical speeds of several tens of km s^{-1} (Raulin and Klein, 1994).

Stewart et al. (1986) proposed a scenario where magnetic flux emerges within a new active region amongst preexisting magnetic structures. The new flux expands and penetrates into the overlying structures so that reconnection creates links with preexisting active regions and new loops form at successively greater altitudes. Although, this scenario is qualitatively consistent with the above observations, the typical speed of upward expansion (1–2 km s^{-1}) that Stewart et al. (1986) inferred from XUV and radio observations, is somewhat smaller than that required to account for the relative timing of microwaves, nonthermal X-rays and metric radio emission at a noise storm onset. More recently, Bentley et al. (2000) have shown that the space and time evolution of a noise storm was closely related to changes observed in the photospheric magnetogram as moving magnetic features (MMF) which are generally associated with decaying sunspots. Magnetic field extrapolations show that the noise storm emitting sources are located in a complex magnetic field topology associated with the MMFs. Since MMFs are expected to drive magnetic reconnection in such a complex topology, it was suggested that MMFs cause the noise storm. This is the first time that a noise storm could be related to clear changes in the photospheric magnetic field. However, this association is not systematic (there are MMFs without noise storms) so that a larger sample of events have to be analysed in order to establish wether or not all noise storms have accompanying MMFs.

SUMMARY

The long-decimetric and longer wavelength radio spectral and imaging observations outlined in this report emphasized that acceleration of suprathermal electrons may occur in association with a large variety of energy release events related with flares, ejecta of cool and hot material in the chromosphere and low corona and the quasi-steady evolution of the global magnetic structure surrounding non-flaring active regions. These various events correspond to a large range of rates of energy release in electrons, i.e.: from 10^{23}–10^{25} erg s^{-1} at $\sim$ 10 keV for noise storms up to $\sim 10^{32}$ erg s^{-1} above 20 keV for giant flares (Kane et al., 1995). The time scales over which electron production operates is also highly variable ($\leq$ 1 s for beams and spikes to several days for noise storms) and acceleration sites are spread over a large domain of altitudes ranging from $\sim 10^3$–10^4 km to more than 1 $R_\odot$ above the photosphere. Despite these large differences the acceleration shares the following characteristics:

- Irrespective of whether the event is part of a flare or not, electron beams are a basic ingredient suggesting that energy release is fragmented (e.g. Bastian and Vlahos, 1997). Narrow band bursts such as spikes and type I which occur on shorter time scales may be further evidence for fragmentation.

- There is strong evidence that electron acceleration is driven by magnetic reconnection in response to changing conditions in the low atmosphere such as the emergence of a new magnetic flux, loop-loop interaction or moving magnetic features.

- The large scale structure of the magnetic field surrounding the sites of acceleration plays a major role in determining the characteristics of the populations of suprathermal electrons.

While acceleration processes operate on short time scales and within small volumes which cannot be resolved by imaging observations, their repetitive occurrence and their distribution within large scale magnetic structures make the global phenomenon extended in space and time. The coupling between the evolution of large scale structures and small scale energy release is not yet understood although it is a crucial issue to set a realistic model of acceleration (cf. Miller et al. 1997). Progress in understanding this coupling will be a major issue for RHESSI. In particular, one should benefit from the enhanced time, spatial and spectral resolution of the XR/GR RHESSI imaging and spectral observations to further investigate the link between spatial and spectral variability during flares and to look for nonthermal X-ray counterparts of small energy release events in the corona. The examples discussed in this paper have also clearly emphasized the potential of radio imaging observations in investigating the physics of electron acceleration during and outside flares. Even if a quantitative understanding of many radio phenomena remains elusive, radio imaging provides a unique way to probe nonthermal energy release events in the corona. However, such observations are, at present, performed routinely only at a few frequencies in the microwave and metric domains. In particular, there are no imaging observations in the decimetric wavelength range, although they are needed to probe the electron acceleration region(s) during flares and to obtain signatures of an energy release event over the whole range of altitudes where it operates. These gaps in radio imaging observations should be removed by the Frequency Agile Solar Radiotelescope (Gary et al., 2001) which is planned to perform images, with high time and spatial resolution, at a large number of radio wavelengths ranging from microwaves to metric waves.

ACKNOWLEDGEMENTS

The author thanks the organisers of the COSPAR session E2.3 for their invitation to give this paper. He is also indebted to Dr. K.-L. Klein for helpful discussions and comments.

REFERENCES

Aschwanden, M., J., Particle acceleration and kinematics in solar flares, *Space Science Rev.*, **101**, 63–68, 2002.

Aschwanden, M. J., A. O. Benz, B. R. Dennis, and R. A. Schwartz, Solar Electron beams detected in hard X-rays and radio waves, *ApJ*, **455**, 347–365, 1995.

Aulanier, G., E. E. DeLuca, S. K. Antiochos, et al., The topology and evolution of the Bastille day flare, *ApJ*, **540**, 1126–1142, 2000.

Aurass, H., K.-L. Klein, and P. C. H. Martens, First detection of correlated electron beams and plasma jets in radio and soft X-ray data, *Solar Phys.*, **155**, 203–206, 1994.

Axisa, F., M.-J. Martres, M. Pick, and I. Soru-Escaut, On some transient Hα features associated with metric type III bursts, *Solar Phys.*, **29** 163–182, 1973.

Bentley, R., D., K.-L. Klein, L. van Driel-Gesztelyi, et al., Magnetic activity associated with radio noise storms, *Solar Phys.*, **193**, 227–245, 2000.

Benz, A. O., and S. R. Kane, Electron acceleration in flares inferred from radio and hard X-ray emissions, *Solar Phys.*, **104**, 179–185, 1986.

Benz, A., O., A. Csillaghy, and M. J. Aschwanden, Metric spikes and electron acceleration in the solar corona, *A&A*, **309**, 291–300, 1996.

Carbone, V., P. Veltri, and G. Einaudi, Effects of turbulence development in surges, *Solar Phys.*, **111**, 31–44, 1987.

Chiuderi-Drago, F., N. Mein, and M. Pick, Unstable chromospheric dark features and type-III burst association, *Solar Phys.*, **103**, 235–247, 1986.

Chupp, E. L., G. Trottet, H. Marschhaüser, et al., A study of the evolution of electron and ion acceleration during the 09:09 UT solar flare on 1989 September 9, *A&A*, **275**, 602–612, 1993.

Cliver, E. and S. Kahler, High coronal flares and impulsive acceleration of solar energetic particles, *ApJ*, **366**, L91–L94, 1991.

Crosby, N., N. Vilmer, N. Lund, et al., Deka-keV X-ray emission associated with the onset of radio noise storms, *Solar Phys.*, **167**, 333–348, 1996.

Elgarøy, Ø., *Solar Noise Storms*, Pergamon Press, Oxford, 1977.

Gary, D. E., T. S. Bastian, S. M. White, and G. J. Hurford, The frequency-agile solar radiotelescope (FASR) (Abstract), *AP-RASC-01*, 236–236, 2001.

Gopalswamy, N., M. R. Kundu, P. K. Manoharan, et al., X-ray and radio studies of a coronal eruption shock wave, plasmoid, and coronal mass ejection, *ApJ*, **486**, 1036–1044, 1997.

Gubchenko, V. M., and V. V. Zaitsev, The source model for low-energy electrons responsible for type I and Type III radio noise storms, *Solar Phys.*, **89**, 391–402, 1983.

Hanaoka, Y., Radio and X-ray observations of the flares caused by interacting loops, *Proceedings of the Nobeyama Symposium, held in Kiyosato, Japan, Oct. 27–30, 1998*, eds. T. S. Bastian, N. Gopalswamy and K. Shibasaki, *NRO Report*, **No 479**, 229–234, 1999.

Kai, K., D. B. Melrose, and S. Suzuki, Storms, in *Solar Radiophysics*, Cambridge University Press, Cambridge and New-York, 415–441, 1985.

Kane, S. R., K. Hurley, J. M. McTiernan, et al., Energy release and dissipation during giant solar flares, *ApJ*, **446**, L47–L50, 1995.

Kerdraon, A., M. Pick, G. Trottet, et al., The association of radio noise storm enhancements with the appearance of additional material in the corona, *ApJ*, **265**, L19–L21, 1983.

Klein, K.-L., Long duration non-thermal energy release in flares and outside flares, in *Coronal Magnetic Energy Release*, eds. A., O. Benz and A. Krüger, *Lecture Notes in Physics*, **444**, 55–74, 1994.

Klein, K.-L., Suprathermal electrons in non-flaring active regions, in *Three-Dimensional Structure of Solar Active Region*, eds. C. E. Alissandrakis and B. Schmieder, *ASP Conf. Ser.*, **155**, 182–201, 1998.

Klein, L., K., M. Pick, G. Trottet, et al., Association between gradual hard X-ray emission and metric continuua during large flares, *Solar Phys.*, **84**, 295–310, 1983.

Klein, K.-L., G. Trottet, A. O. Benz, and S. R. Kane, Extended coronal shock waves and electron acceleration during solar flares, in *Proceedings of an International School and Workshop on Plasma Astrophysics*, ESA Publications Division, ESTEC, Noordwijk, The Netherlands, eds. T. D. Guyenne and J. J. Hunt, *ESAP SP*, **285 Vol 1**, 157–160, 1989.

Klein, K.-L., H. Aurass, I. Soru-Escaut, and B. Kálmán, Electron acceleration sites in large-scale coronal structure, *A&A*, **320**, 612-619, 1997. (Erratum with correctly printed figure in *A&A*, **322**, 1027–1027)

Klein, K.-L., E. Chupp, G. Trottet, et al. , Flare associated energetic particles in the corona and at 1 AU, *A&A*, **348**, 271–285, 1999a.

Klein, K.-L., J. I. Khan, N. Vilmer, J.-M. Delouis, and H. Aurass, X-ray and radio evidence of the origin of a coronal shock wave, *A&A*, **346**, L53–L56, 1999b.

Klein, K.-L. and G. Trottet, The origin of solar energetic particle events: coronal acceleration versus shock wave acceleration, *Space Science Rev.*, **95**, 215–225, 2001.

Klein, K.-L., G. Trottet, P. Lantos, and J.-P. Delaboudinière, Coronal electron acceleration and relativistic proton production during the 14 July 2000 flare and CME, *A&A*, **373**, 1073–1082, 2001.

Klein, K.-L. and Z. Mouradian, The dynamics of an eruptive prominence, *A&A*, **381**, 683–693, 2002.

Kundu, M., R., J.-P. Raulin, M. Pick, and K., T. Strong, Metric type III bursts from a flaring X-ray bright point near an active region, *ApJ*, **444**, 922–928, 1995.

Kundu, M. R., N. Nindos, N. Vilmer, et al., Metric radio emission associated with X-ray plasmoid ejections, *ApJ*, **559**, 443–451, 2001.

Krucker, S., M. J. Aschwanden, T. S. Bastian, and A. O. Benz, First VLA observation of a narrowband millisecond spike event, *A&A*, **302**, 551–563, 1995.

Krucker, S., A. O. Benz, and M. J. Aschwanden, YOHKOH observation of the source regions of solar narrowband millisecond spike events, *A&A*, **317**, 569–579, 1997.

Krucker, S., and R. P. Lin, Relative timing and spectra of solar flare hard X-ray sources, *Solar Phys.*, **210**, 229–243, 2002.

Laitinen, T., K.-L. Klein, L. Kocharov, et al., Solar energetic particle events and radio bursts associated with the 1996 July 9 flare and coronal mass ejection, *A&A*, **360**, 729–741, 2000.

Lin, R. P., Energetic solar electrons in the interplanetary medium, *Solar Phys.*, **100**, 537–561, 1985.

Lin, R. P., Observations of the 3D distributions of thermal to near-relativistic electrons in the interplanetary medium by the WIND spacecraft, in *Coronal Physics from Radio and Space Observations*, ed. G. Trottet, *Lecture Notes in Physics*, **483**, 93–107, 1997.

Maia, D., A. Vourlidas, M. Pick, et al., Radio signatures of a fast coronal mass ejection development on November 6, 1997, *JGR*, **104**, 12507–12514, 1999.

Miller, J. A., P. A. Cargill, A. G. Emslie, et al., Critical issues for understanding particle acceleration in impulsive solar flares, *JGR*, **102**, 14631–14660, 1997.

Paesold, G., A. O. Benz, K.-L. Klein, and N. Vilmer, Spatial analysis of solar type III events associated with narrow band spikes at metric wavelengths, *A&A*, **371**, 333–342, 2001.

Pick, M., Observations of radio continua and terminology, *Solar Phys.*, **104**, 19–32, 1986.

Raoult, A., M. Pick, and B. R. Dennis, Solar flare development during the impulsive phase as deduced from correlated radio and hard X-ray observations, *ApJ*, **299**, 1027–1035, 1985.

Raulin, J.-P., R. F. Willson, A. Kerdraon, et al., Acceleration of electrons outside flares - Coronal manifestations and possible origin, *A&A*, **251**, 298–306, 1991.

Raulin, J.-P. and K.-L. Klein, Acceleration of electrons outside flares: Evidence for coronal evolution and height-extended energy release during noise storms, *A&A*, **281**, 536–550, 1994.

Raulin, J.-P., M. R. Kundu, H. S. Hudson, N. Nitta, and A. Raoult, Metric type III bursts associated with soft X-ray jets, *A&A*, **306**, 299–304, 1996.

Raulin, J.-P., N. Vilmer, G. Trottet, et al., Small and large scale magnetic structures involved in the development of the 1992 October 28 solar flare, *A&A*, **355**, 355–364, 2000.

Rieger, E., R. A. Treumann, and M. Karlicky, The radio silent start of an intense solar gamma-ray flare, *Solar Phys.*, **187**, 59–75, 1999.

Sakao, T., T. Kosugi, S. Masuda, et al., Hard X-ray imaging observations by Yohkoh of the 1991 November 15 solar flare, *PASJ*, **44**, L83–L87, 1992.

Simnett, G. M. and A. O. Benz, The role of metric and decimetric radio emission in the understanding of solar flares, *A&A* **165**, 227–234, 1986.

Shibata, K., Rapidly time variable phenomena: jets, explosive events, and flares, in *Fifth SOHO Workshop: The Corona and Solar Wind Near Minimum Activity*, eds. A. Wilson, *ESA-SP*, **404**, 103–112, 1997.

Stewart, R. T., G. E. Brueckner, and K. P. Dere, Culgoora radio and SKYLAB EUV observations of emerging magnetic flux in the lower corona, *Solar Phys.*, **106**, 107–130, 1986.

Švestka, Z. and E. W. Cliver, Historic and basic characteristics of eruptive flares, in *Eruptive Solar Flares, Proceedings of Colloquium # 113 of the International Astronomical Union, held at Iguazu, Argentina, August 2–6, 1991*, Springer-Verlag, New-York, eds. Z. Švestka, B. V. Jackson and M. E. Machado, pp. 1–14, 1992.

Takakura, T., M. Inda, K. Makishima, et al., Time variation of the hard X-ray image during the early phase of solar impulsive bursts, *PASJ*, **45**, 737–753, 1993.

Trottet, G., Relative timing of hard X-rays and radio emissions during the different phases of solar flares: consequences for the electron acceleration, *Solar Phys.*, **104**, 145–163, 1986.

Trottet, G., E. L. Chupp, H. Marschhaüser, et al., A comparison of gamma-ray and radio emissions during the 11:42 UT solar flare on 1982 June 3, *A&A*, **288**, 647–655, 1994.

Trottet, G., and N. Vilmer, The production of flare-accelerated particles at the Sun, in *Solar and Heliospheric Plasma Physics*, eds. G. M. Simnett, C. E. Alissandrakis and L. Vlahos, *Lecture Notes in Physics*, **489**, 219–239, 1997.

Trottet, G., N. Vilmer, C. Barat, et al., A multiwavelength analysis of an electron-dominated gamma-ray event associated with a disk solar flare, *A&A*, **334**, 1099–1111, 1998.

van Driel-Gesztelyi, L., R. F. Willson, J. N. Kile, et al., X-ray jets and their radio signatures at metric and centimetric wavelengths, in *The Tenth Cambridge Workshop on Cool Stars, Stellar Systems and the Sun*, eds. R. A. Donahue and A. Bookbinder, *ASP Conf. Ser.*, **154**, 707–717, 1998.

Vilmer, N., and G. Trottet, Solar flare radio and hard X-ray observations and the avalanche model, in *Coronal Physics from Radio and Space Observations*, ed. G. Trottet, *Lecture Notes in Physics*, **483**, 28–52, 1997.

Vilmer, N., S. Krucker, R. P. Lin, et al., Hard X-ray and metric/decimetric radio observations of the 20 February 2002 solar flare, *Solar Phys.*, **210**, 261-272, 2002.

E-mail address of G. Trottet gerard.trottet@obspm.fr

Manuscript received 29 November 2002; revised 24 February, 2003; accepted 24 February, 2003